Electronic Supplementary Information

Zn_2Yb-grafted and star-shaped metallopolymer for efficient near-infrared (NIR) polymer light-emitting diode (PLED)

Guorui Fu, Yani He, Baoning Li, Lin Liu, Wentiao Li, Zhao Zhang and Xingqiang Lü*

Supporting information

Materials and methods

High performance liquid chromatography (HPLC)-grade THF or MeCN was purchased from Fisher Scientific and purified over solvent columns. Other solvents were used as received from Sigma Aldrich and stored over 3 Å activated molecule sieves. 5-Allyl-2-hydroxy-3-methoxy-benzaldehyde was synthesized according to a well-established procedure from the literature.[1] Other chemicals containing Hoveyda-Grubbs II (H-Grubbs II) and NBE (norbornene) were commercial products of reagent grade and were used without further purification. All manipulations of air and water sensitive compounds were carried out under dry N_2 using the standard Schlenk line techniques.

Elemental analyses were performed on a Perkin-Elmer 240C elemental analyzer. Fourier Transform Infrared (FT-IR) spectra were recorded on a Nicolet Nagna-IR 550 spectrophotometer in the region 4000-400 cm^{-1} using KBr pellets. ^1H NMR spectra were recorded on a JEOL EX 400 spectrometer with $SiMe_4$ as internal standard in DMSO-d_6 and/or

$CDCl_3$ or CD_3CN at room temperature. ESI-MS was performed on a Finnigan LCQ^{DECA} XP HPLC-MS_n mass spectrometer with a mass to charge (*m/z*) range of 4000 using a standard electro-spray ion source and MeCN as the solvent. Electronic absorption spectra in the UV/Visible region and diffuse reflection (DR) spectra were recorded with a Cary 300 UV spectrophotometer. Visible or NIR emission and excitation spectra were collected by a combined fluorescence lifetime and steady-state spectrometer (FLS-980, Edinburgh) with a 450 W Xe lamp. Excited-state decay times were obtained by the same spectrometer but with a μF900 Xe lamp. The luminescent absolute overall quantum yield (Φ_{Ln}^{L}) was determined by the same spectrometer using a 450 W Xe lamp and an integrating sphere. Gel permeation chromatography (GPC) analyses of the polymers were performed using a Waters 1525 binary pump coupled to a Waters 2414 refractive index detector with HPLC THF as the eluant on American Polymer Standard 10 μm particle size, linear mixed bed packing columns. The GPC was calibrated using polystyrene standards. X-ray photoelectron spectroscopy (XPS) was carried out on a PHI 5700 XPS system equipped with a dual Mg X-ray source and monochromatic Al X-ray source with the complete depth profile and angle-resolved capabilities. Powder X-ray diffraction (PXRD) patterns were recorded on a D/Max-IIIA diffractometer with graphite-monochromatized Cu Kα radiation (λ = 1.5418 Å). Thermal properties were characterized using Thermogravimetric (TG) and differential scanning calorimetry (DSC) analyses on a NETZSCH TG 209 instrument under flowing nitrogen at a heating rate of 10 °C/min.

Synthesis of the allyl-functionalized benzimidazole-type ligand HL (HL = 4-allyl-2-(1*H*-

benzo[*d*]imidazol-2-yl)-6-methoxyphenol)

To a stirred solution of *o*-phenylenediamine (0.55 g, 5 mmol) in absolute MeOH (20 mL), 5-allyl-2-hydroxy-3-methoxy-benzaldehyde (1.92 g, 10 mmol) was added, and the resultant mixture was refluxed under an N_2 atmosphere for 36 h. During the reaction, the color of the solution changed from dark red to brown and to white. After cooling to room temperature, the resulting off-white microcrystalline precipitate was filtered off, and washed with absolute MeOH and diethyl ether and further dried under vacuum. Yield: 0.785 g (56%). Calc. for $C_{17}H_{16}N_2O_2$: C, 72.84; H, 5.75; N 9.99%. Found: C, 72.75; H, 5.58; N, 10.05%. FT-IR (KBr, cm^{-1}): 3464 (b), 3067 (w), 2970 (w), 2928 (w), 2293 (w), 2259 (w), 2212 (w), 1634 (m), 1599 (m), 1499 (s), 1454 (s), 1398 (s), 1342 (m), 1254 (vs), 1146 (s), 1063 (s), 997 (m), 964 (w), 914 (m), 851 (m), 800 (m), 748 (m), 681 (w), 615 (m), 548 (w), 494 (w), 434 (w). ^{1}H NMR (400 MHz, CD_3CN):δ (ppm) 12.99 (s, 1H, -NH), 11.09 (s, 1H, -OH), 7.72 (d, 1H, -Ph), 7.60 (d, 1H, -Ph), 7.31 (m, 3H, -Ph), 6.94 (s, 1H, -Ph), 6.09 (m, 1H, -CH=), 5.17 (m, 2H, $=CH_2$), 3.90 (s, 3H, -OMe), 3.44 (d, 2H, $-CH_2$).

Characterization of complex monomers 2-5

For complex monomer **2**: Yield: 0.171 g (73%). Calc. for $C_{72}H_{66}N_9O_{15}Zn_2Nd$: C, 55.00; H, 4.23; N, 8.02%. Found: C, 54.92; H, 4.34; N, 8.07%. FT-IR (KBr, cm^{-1}): 3207 (w), 2971 (w), 2426 (w), 1653 (s), 1628 (m), 1600 (m), 1564 (m), 1534 (s), 1491 (s), 1462 (m), 1454 (s), 1426 (s), 1385 (vs), 1349 (s), 1312 (s), 1285 (m), 1252 (s), 1202 (m), 1148 (m), 1118 (w), 1062 (m), 1020 (m), 1001 (m), 962 (w), 912 (m), 866 (m), 854 (w), 820 (m), 768 (m), 745 (m), 684 (w), 663 (w), 625 (w), 579 (w), 510 (w), 456 (w). ESI-MS (in MeCN) *m*/*z*: 1510.24 (100%; $[M-(NO_3)]^+$).

For complex monomer **3**: Yield: 0.158 g (66%). Calc. for $C_{72}H_{66}N_9O_{15}Zn_2Yb$: C, 54.01; H, 4.15; N, 7.87%. Found: C, 54.05; H, 4.28; N, 7.81%. FT-IR (KBr, cm^{-1}): 3203 (w), 2975 (w), 2425 (w), 1646 (s), 1625 (m), 1598 (m), 1567 (m), 1534 (s), 1494 (s), 1458 (m), 1448 (s), 1430 (s), 1384 (vs), 1350 (s), 1310 (s), 1284 (m), 1251 (s), 1204 (m), 1151 (m), 1120 (w), 1064 (m), 1020 (m), 1004 (m), 963 (w), 912 (m), 867 (m), 853 (w), 821 (m), 767 (m), 745 (m), 685 (w), 663 (w), 632 (w), 579 (w), 514 (w), 462 (w). ESI-MS (in MeCN) *m*/*z*: 1538.33 (100%; $[M-(NO_3)]^+$).

For complex monomer **4**: Yield: 0.155 g (65%). Calc. for $C_{72}H_{66}N_9O_{15}Zn_2Er$: C, 54.20; H, 4.17; N, 7.90%. Found: C, 54.12; H, 4.29; N, 7.93%. FT-IR (KBr, cm^{-1}): 3201 (w), 2974 (w), 2425 (w), 1648 (s), 1626 (m), 1601 (m), 1569 (m), 1534 (s), 1494 (s), 1460 (m), 1449 (s), 1430 (s), 1385 (vs), 1350 (s), 1313 (s), 1282 (m), 1251 (s), 1204 (m), 1149 (m), 1118 (w), 1063 (m), 1020 (m), 1002 (m), 963 (w), 914 (m), 868 (m), 854 (w), 820 (m), 767 (m), 744 (m), 685 (w), 661 (w), 632 (w), 578 (w), 514 (w), 461 (w). ESI-MS (in MeCN) *m*/*z*: 1532.34 (100%; $[M-(NO_3)]^+$).

For complex monomer **5**: Yield: 0.166 g (70%). Calc. for $C_{72}H_{66}N_9O_{15}Zn_2Gd$: C, 54.55; H, 4.20; N, 7.95%. Found: C, 54.48; H, 4.37; N, 7.93%. FT-IR (KBr, cm^{-1}): 3203 (w), 2975 (w), 2429 (w), 1649 (s), 1629 (m), 1601 (m), 1562 (m), 1535 (s), 1492 (s), 1463 (m), 1452 (s), 1425 (s), 1383 (vs), 1350 (s), 1310 (s), 1281 (m), 1252 (s), 1203 (m), 1147 (m), 1122 (w), 1064 (m), 1021 (m), 1003 (m), 960 (w), 914 (m), 867 (m), 857 (w), 820 (m), 771 (m), 746 (m), 689 (w), 668 (w), 631 (w), 582 (w), 514 (w), 453 (w). ESI-MS (in MeCN) *m*/*z*: 1522.33 (100%; $[M-(NO_3)]^+$).

X-ray crystallography

Single crystals for complex monomer **2** of suitable dimensions were mounted onto thin glass

fibers. All the intensity datas were collected on a Bruker SMART CCD diffractometer (Mo-Kα radiation and λ = 0.71073 Å) in Φ and ω scan modes. Structures were solved by Direct methods followed by difference Fourier syntheses, and then refined by full-matrix least-squares techniques against F^2 using SHELXTL.[2] All other non-hydrogen atoms were refined with anisotropic thermal parameters. Absorption corrections were applied using SADABS.[3] All hydrogen atoms were placed in calculated positions and refined isotropically using a riding model. Crystallographic data, relevant atomic distances and bond angles for the complex monomer **2** are presented in Tables 1-2S, respectively. CCDC number 1526559 for complex monomer **2**.

Synthesis of PNBE in activation with H-Grubbs II

To a solution of NBE (70 mg, 0.75 mmol) in absolute $CHCl_3$ (15 mL), H-Grubbs II initiator (1.1 mg, 1.5 mol-% of NBE) was added in three times (0.6 mg, 0.3 mg and 0.2 mg), and the resultant mixture was purged with N_2 for 10 min and sealed under a reduced N_2 atmosphere. After the homogeneous solution was continuously stirred at room temperature for 48 h, ethyl vinyl ether (100 μL) was added to quench the reaction. The viscous mixture was diluted with absolute THF (20 mL) and dried at 45 ^{o}C under vacuum to constant weight. For PNBE: Yield: 92%. FT-IR (KBr, cm^{-1}): 2924 (m), 2853 (s), 1944 (w), 1450 (s), 1432 (s), 1401 (w), 1370 (w), 1346 (w), 1303 (w), 1180 (w), 1069 (w), 1028 (w), 996 (w), 941 (w), 735 (s), 698 (vs), 540 (w).^{1}H NMR (400 MHz, DMSO-d_6): δ (ppm) 5.35 (s, =CH-), 2.40 (s, -CH), 1.83 (m, $-CH_2$), 1.28 (m, $-CH_2$), 1.01 (m, $-CH_2$).

Characterization of PNBE-supported metallopolymers based on complex monomers 2-5

For **Poly(2-*co*-NBE)** (1:400): Yield: 79%. FT-IR (KBr, cm^{-1}): 3645 (w), 3302 (w), 2992 (m), 2947 (s), 2862 (m), 2313 (w), 1712 (m), 1613 (w), 1554 (s), 1493 (vs), 1452 (s), 1348 (m), 1306 (s), 1260 (s), 1026 (m), 963 (s), 912 (m), 824 (w), 740 (m), 663 (w), 599 (w), 527 (w), 496 (w), 447 (w). XPS data: molar ratio of 2.04:1 *vs* $[Zn^{2+}]/[Nd^{3+}]$.

For **Poly(3-*co*-NBE)** (1:200, 1:400 or 1:800): Yield: 64% (1:200); 81% (1:400); 86% (1:800). FT-IR (KBr, cm^{-1}): 3641 (w), 3300 (w), 2991 (m), 2943 (s), 2862 (m), 2316 (w), 1711 (m), 1612 (w), 1550 (s), 1493 (vs), 1450 (s), 1350 (m), 1310 (s), 1258 (s), 1026 (m), 966 (s), 908 (m), 824 (w), 741 (m), 665 (w), 599 (w), 527 (w), 496 (w), 442 (w). Molar ratio of 2.05:1 (1:200); 2.06:1 (1:400) or 2.08:1 (1:800) *vs* $[Zn^{2+}]/[Yb^{3+}]$.

For **Poly(4-*co*-NBE)** (1:400): Yield: 79%. FT-IR (KBr, cm^{-1}): 3652 (w), 3302 (w), 2992 (m), 2943 (s), 2860 (m), 2316 (w), 1712 (m), 1612 (w), 1546 (s), 1493 (vs), 1452 (s), 1350 (m), 1304 (s), 1261 (s), 1028 (m), 967 (s), 910 (m), 823 (w), 740 (m), 665 (w), 604 (w), 527 (w), 498 (w), 446 (w). XPS data: molar ratio of 1.98:1 *vs* $[Zn^{2+}]/[Er^{3+}]$.

For **Poly(5-*co*-NBE)** (1:400): Yield: 79%. FT-IR (KBr, cm^{-1}): 3646 (w), 3307 (w), 2993 (m), 2943 (s), 2862 (m), 2313 (w), 1711 (m), 1610 (w), 1552 (s), 1493 (vs), 1452 (s), 1348 (m), 1308 (s), 1260 (s), 1024 (m), 966 (s), 910 (m), 824 (w), 742 (m), 665 (w), 598 (w), 527 (w), 498 (w), 449 (w). XPS data: molar ratio of 2.01:1 *vs* $[Zn^{2+}]/[Gd^{3+}]$.

Cyclic voltammetry (CV) measurement

Cyclic voltammetry (CV) measurementwas performed on a computer-controlled EG&G Potentiostat/Galvanostat model 283 at room temperature with a conventional three-

electrode cell using using a an $Ag/AgNO_3$ (0.1 M) reference electrode, Pt carbon working electrode of 2 mm in diameter, and a platinum wire counter electrode. CV of the sample was performed in nitrogen-saturated dichloromethane containing 0.1 M Bu_4NPF_6 as supporting electrolyte. The cyclic voltammogramwas measured at a scan rate of 100 $mV \cdot s^{-1}$. The highest occupied molecular orbit (HOMO) and the lowest unoccupied molecular orbit (LUMO) energy levels of **Poly(3-*co*-NBE)** (1:200) are calculated according to the following equations,[4] $E_{HOMO} = -(E_{OXD} - E_{OXD,\ ferrocene}) - 4.8$ eV, $E_{LUMO} = E_{HOMO} + E_g$ eV, and where E_g is the energy band gap estimated from the low-energy edge of the absorption spectra from the samples. The HOMO and LUMO energy levels for the other used materials were obtained from the literatures.[5]

NIR-PLEDs' fabrication and testing

Each of the two NIR-PLEDs **A**-**B** was fabricated on ITO (Indium tin oxide) coated glass substrates with a sheet resistance of 20 Ω per square. Patterned ITO coated glass substrates were washed with acetone, detergent, D. I. water and isopropanol in an ultrasonic bath. After being exposed under oxygen plasma for 20 min, PEDOT:PSS from water solution was spin-coated (at 2000 rpm) on the substrate and followed by drying in a vacuum oven at 140 °C for 20 min, giving a film of 30 nm thickness. The toluene solution (5 mg/mL) of **Poly(3-*co*-NBE)** (1:200) as the emitting layer was prepared under an N_2 atmosphere and spin-coated (at 3000 rpm) on the PEDOT:PSS layer with a thickness of 40 nm. Subsequently, the TPBI layer (20 nm) and/or the BCP layer (20 nm) were thermally deposited onto the emitting layer for NIR-PLEDs **A**-**B**, respectively. Finally, a thin layer (1 nm) followed by 100 nm thickness Al

capping layer was deposited onto the substrate under vacuum of 5×10^{-6} Pa. Current density-voltage characteristics were collected using a Keithley 2400 source meter equipped with a calibrated silicon photodiode. The NIR EL irradiance was measured through a calibrated UDT Model 280 Germanium Detector. The eternal quantum efficiencies (EQEs) of the NIR emission were obtained by measuring the irradiance in the forward direction and assuming the eternal emission profile to Lambertian.

References

1 Z. Zhang, H. N. Feng, L. Liu, C. Yu, X. Q. Lü, X. J. Zhu, W.-K. Wong, R. A. Jones, M. Pan and C. Y. Su, *Dalton Trans.*, 2015, 44, 6229-6241.

2 G. M.Sheldrick, *SHELXL-97*, Program for Crystal Structure Refinement, University of Göttingen, Göttingen, Germany, 1997.

3 G. M. Sheldrick, *SADABS*, University of Göttingen, Göttingen, Germany, 1996.

4 H. Y. Chen, C. T. Chen and C. T. Chen, *Macromolecules,* 2010, 43, 3613-3623.

5 E. Zysman-Colman, S. S. Ghosh, G. Xie, S. Varghese, M. Chowdhury, N. Sharma, D. B. Cordes, A. M. Z. Slawin and I. D. W. Samuel, *ACS Appl. Mater. & Interfaces,* 2016, 8, 9247-9253.

Table 1S. Crystal data and structure refinement for complex monomer **2**.

Compound	**2**
Empirical formula	$C_{72}H_{66}N_9O_{15}Zn_2Nd$
Formula weight	1572.35
Crystal size/mm	0.32 ×0.28 ×0.25
T/K	296.15
λ/Å	0.71073
Crystal system	Monoclinic
Space group	*P2(1)/c*
a/Å	19.0281(18)
b/Å	17.4257(17)
c/Å	26.483(3) A
α/°	90
β/°	108.859(2)
γ/°	90
V/Å^3	8309.8(15)
Z	4
ρ/mg·m^{-3}	1.257
μ/mm^{-1}	1.249
F(000)	3204
Data/restraints/parameters	14872/1209/898
Quality-of-fit indicator	0.873
Final *R* indices [*I*>2σ(*I*)]	R_1 = 0.0761
	$_wR_2$ = 0.1845
R indices (all data)	R_1 = 0.1970
	$_wR_2$ = 0.2402

Table 2S. Selected inter-atomic distance (Å) and bond angles (°) with esds for complex monomer **2**.

Compound	**2**		
Zn(1)-N(1)	2.080(9)	Zn(1)-N(3)	2.038(9)
Zn(1)-O(2)	2.051(7)	Zn(1)-O(4)	2.084(7)
Zn(1)-O(12)	2.000(8)	Zn(2)-N(5)	2.042(8)
Zn(2)-N(7)	2.020(8)	Zn(2)-O(6)	2.015(6)
Zn(2)-O(8)	2.118(7)	Zn(2)-O(9)	1.989(7)
Nd(1)-O(1)	2.768(7)	Nd(1)-O(2)	2.430(6)
Nd(1)-O(3)	2.911(7)	Nd(1)-O(4)	2.410(7)
Nd(1)-O(5)	2.775(6)	Nd(1)-O(6)	2.421(6)
Nd(1)-O(7)	2.708(8)	Nd(1)-O(8)	2.434(7)
Nd(1)-O(10)	2.429(8)	Nd(1)-O(11)	2.434(8)
C(9)-C(10)	1.298(16)	C(26)-C(27)	1.314(13)
C(43)-C(44)	1.319(16)	C(60)-C(61)	1.311(17)
Zn(1)···Nd(1)	3.5311(14)	Zn(2)···Nd(1)	3.5106(13)
Zn(1)-Nd(1)-Zn(2)	167.12(4)		

Table 3S. GPC and XPS data of PNBE and Poly({$[Zn_2(L)_4Ln(OAc)_2]\cdot(NO_3)$}-*co*-NBE) (Ln = La, **1**; Ln = Nd, **2**; Ln = Yb, **3**; Ln = Er, **4**; Ln = Gd, **5**).

Sample	Monomers	[a]Monomer/NBE (feed)	[b]M_n/g·mol	[c]PDI	[d]Zn^{2+}/Ln^{3+}	[d]Monomer/NBE (actual)
PNBE	NBE	-	20199	2.03	-	-
Poly(1-*co*-NBE)	**1** and NBE	1:400	17688	2.33	1.96:1	1:328
Poly(2-*co*-NBE)	**2** and NBE	1:400	17920	2.30	2.04:1	1:320
Poly(3-*co*-NBE)	**3** and NBE	1:200	9960	1.59	2.05:1	1:128
Poly(3-*co*-NBE)	**3** and NBE	1:400	18125	2.29	2.06:1	1:324
Poly(3-*co*-NBE)	**3** and NBE	1:800	28390	2.58	2.09:1	1:680
Poly(4-*co*-NBE)	**4** andNBE	1:400	17821	2.31	1.98:1	1:320
Poly(5-*co*-NBE)	**5** andNBE	1:400	17747	2.34	2.01:1	1:320

[a]The feed molar ratio between monomer and NBE

[b]M_n is the number-average molecular weight, g/mol

[c]PDI = M_w/M_n, where M_w is the weight-average molecular weight, g/mol

[d]The actual Zn^{2+}/Ln^{3+} molar ratio and monomer/NBE determined by XPS

Figure 1S. UV-visible absorption spectra of the ligand **HL** and its complex monomers **2-5** in MeCN solution (1×10^{-5} M).

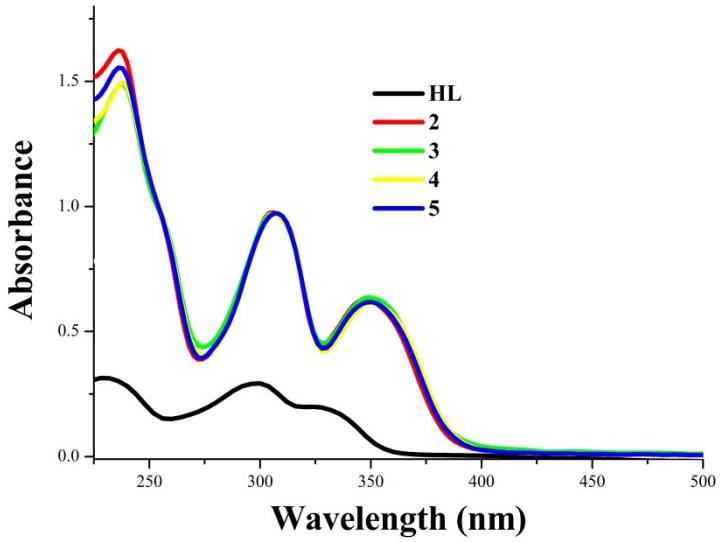

Figure 2S. Visible emission and excitation spectra of complex monomer **5** in MeCN solution (1×10^{-5} M) and **Poly(5-*co*-NBE)**(1:400) in solid state at RT or 77 K.

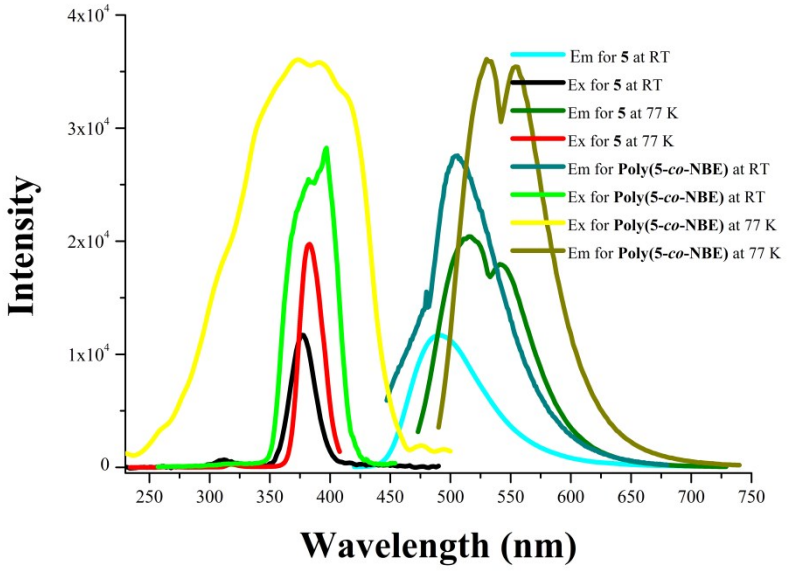

Figure 3S. Schematic energy level diagram and energy transfer process of Nd^{3+}, Yb^{3+} or Er^{3+} for complex monomers {$[Zn_2(L)_4Ln(OAc)_2]\cdot(NO_3)$} (**2**-**4**) and their metallopolymers Poly({$[Zn_2(L)_4Ln(OAc)_2]\cdot(NO_3)$}-*co*-NBE).

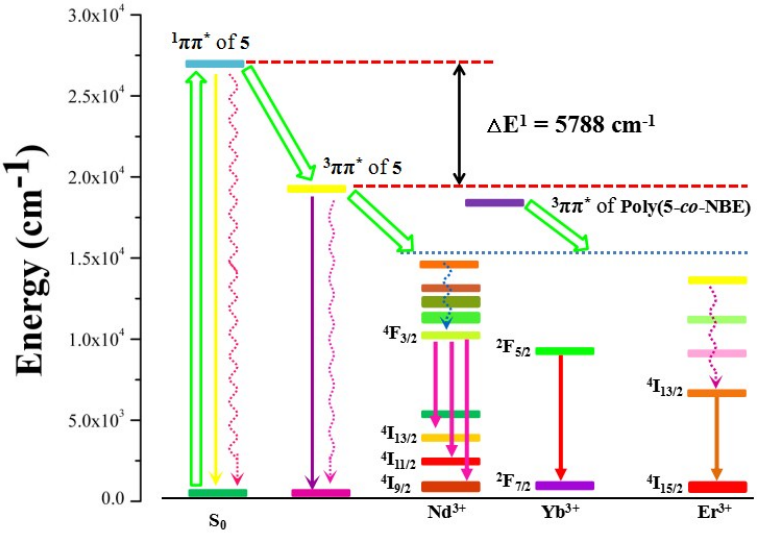

Figure 4S. MALDI-ToF-MS spectrum of the oligomeric metallopolymer **Poly(1-*co*-NBE)** from a stipulated feed molar ratio of 1:400.

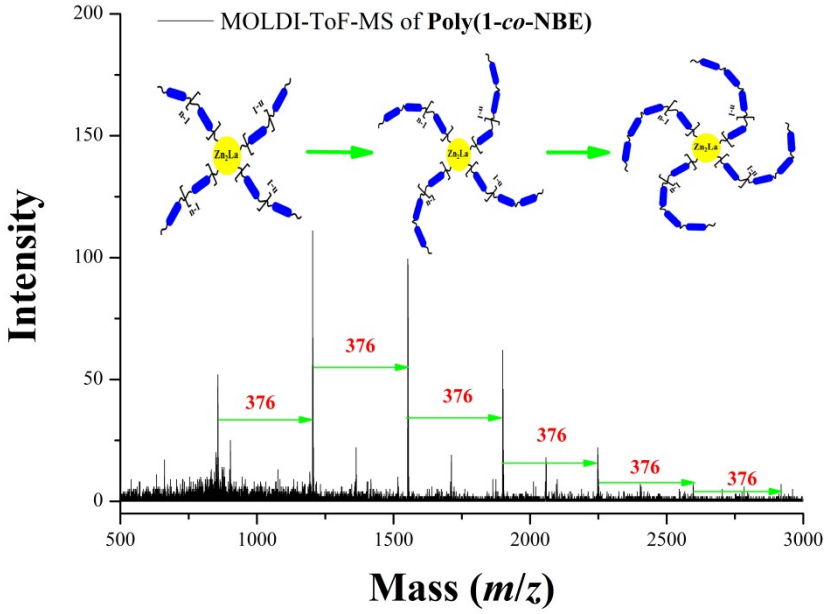

Figure 5S. PXRD patterns of PNBE and the series of Zn_2Ln-containingmetallopolymers **Poly(2-*co*-NBE)**, **Poly(3-*co*-NBE)**,**Poly(4-*co*-NBE)** and **Poly(5-*co*-NBE)**with a stipulated feed molar ratio of 1:400.

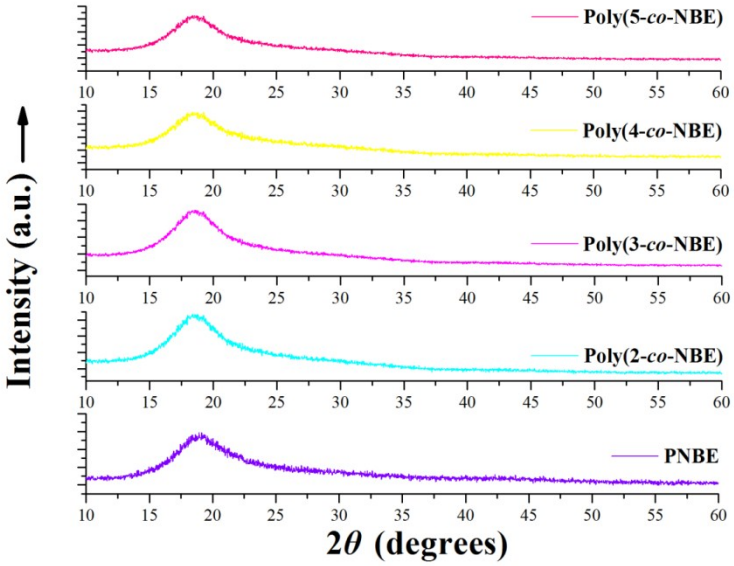

Figure 6S. TG and DSC (inserted; for Poly(3-*co*-NBE) (1:200)) curves of PNBE and the Zn_2Ln-grafted metallopolymers **Poly(1-*co*-NBE)**, **Poly(2-*co*-NBE)**, **Poly(3-*co*-NBE)** and **Poly(4-*co*-NBE)** with a feed molar ratio of 1:400.

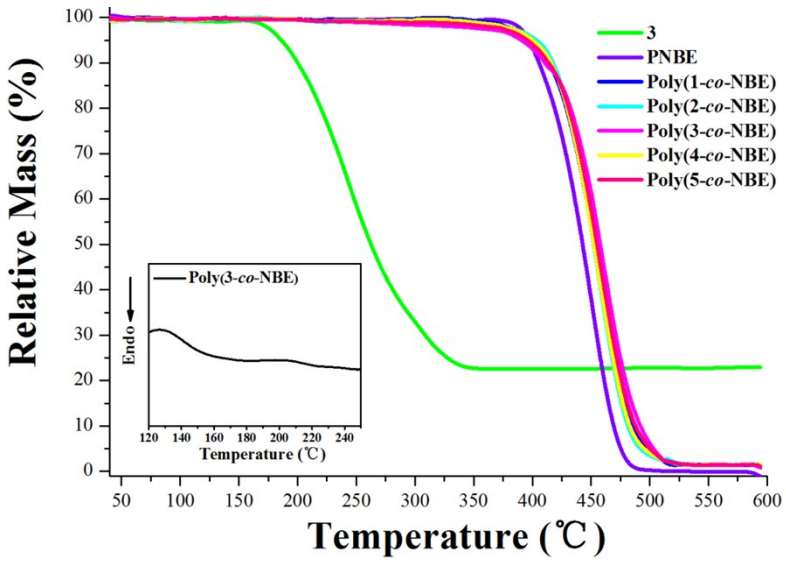

Figure 7S. DR spectra of the Zn_2Ln-containingmetallopolymers **Poly(2-*co*-NBE)**, **Poly(3-*co*-NBE), Poly(4-*co*-NBE)** and **Poly(5-*co*-NBE)** with a stipulated feed molar ratio of 1:400.

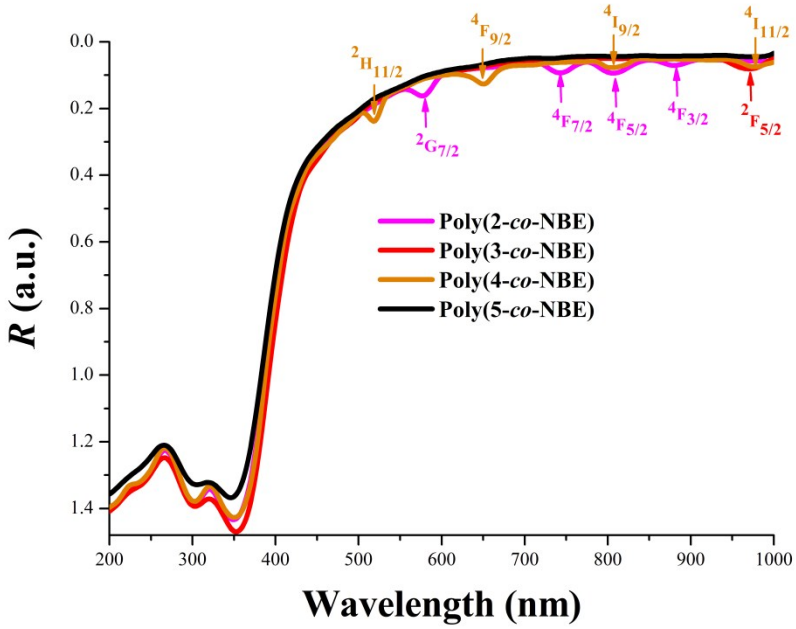

Figure 8S. Overlapping area between the normalized emission spectrum of PNBE and the UV-visible absorption spectrum of complex monomer **3**.

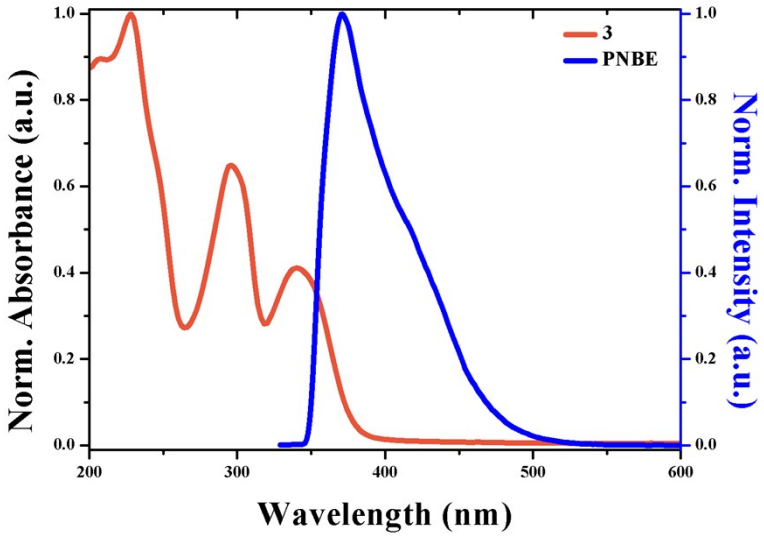

Figure 9S. CV curve of **Poly(3-*co*-NBE)** (1:200) in dilute CH_2Cl_2 solution.

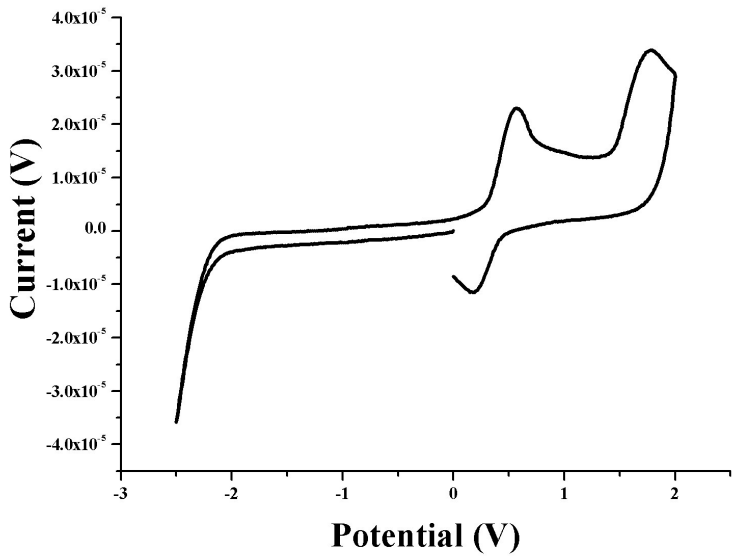

Figure 10S. The curves of current density (mA/cm^2) and irradiance (μW/cm^2) as a function of applied voltage (v) for the two NIR-PLEDs **A** and **B**.